Angiostatic Effect of CXCR3 Expressed on Choroidal Neovascularization

Shigeto Fujimura,[1] *Hidenori Takahashi,*[1] *Kentaro Yuda,*[1] *Takashi Ueta,*[1] *Aya Iriyama,*[1] *Tatsuya Inoue,*[1] *Toshikatsu Kaburaki,*[1] *Yasuhiro Tamaki,*[1] *Kouji Matsushima,*[2] *and Yasuo Yanagi*[1]

Purpose. Several recent studies suggest that some chemokines/chemokine receptors are involved in choroidal neovascularization (CNV). CXCR3 was the focus of the present study because microarray analysis for murine laser-induced CNV model showed the increased expression of CXCR3. The purpose of this study was to evaluate the effect of CXCR3 on CNV.

Methods. Microarray analysis was performed for the mouse eyes with laser-induced CNV. CXCR3 expressions on the CNV were evaluated by immunohistochemistry and real-time RT-PCR. CNV was compared between CXCR3-deficient mice and wild-type mice, between mice treated with anti-CXCR3/anti-IP-10 neutralizing antibody and mice treated with control IgG. Macrophage recruitment into CNV was also investigated. Ocular expressions of vascular endothelial growth factor (VEGF), pigment epithelium-derived factor (PEDF), C-C chemokine ligand-2 (CCL2), and complement component-3 (C3) were evaluated by real-time PCR.

Results. Microarray analysis and real-time RT-PCR revealed the elevation of CXCR3 and IP-10 in laser-treated mouse eyes compared with control eyes. Immunohistochemistry showed CXCR3 expression on the endothelial cells of CNV. Laser-induced CNV of CXCR3-deficient mice was significantly larger, with greater leakage in fluorescein angiography, and with greater macrophage-infiltration compared with wild-type mice ($P < 0.01$). Intravitreal injection of anti-CXCR3/anti-IP-10 neutralizing antibody exacerbated CNV. The CCL2 expression in the laser-treated eyes of CXCR3-deficient mice was higher than in those of wild-type mice ($P < 0.05$), whereas VEGF, PEDF, and C3 showed no differences.

Conclusions. These results suggested that CXCR3 expressed on CNV could have an angiostatic effect on it. (*Invest Ophthalmol Vis Sci.* 2012;53:1999–2006) DOI:10.1167/iovs.11-8232

Choroidal neovascularization (CNV) is the predominant cause of severe visual loss in age-related macular degeneration (AMD) and other macular diseases. CNV formation is considered to be due to an imbalance between angiogenic and angiostatic factors that lead to neovascular growth from the choriocapillaris into subretinal space. Drusen and retinal pigment epithelium (RPE) dysfunction are implicated in CNV formation. A body of evidence suggests that injury to the RPE plays a role in Drusen biogenesis.[1,2] This injury is considered to occur through gene mutations, light damage, oxidative stress, and lipofuscin accumulation, and results in the release of cytokines into Bruch's membrane.[3] Some of the chemokines diffuse into the choroid and work for the inflammatory cells, which amplifies the local inflammatory cycle by mechanisms including immune complex formation and complement activation.[4,5] Thus, chronic inflammation is an important process in Drusen biogenesis.

Chemokines are a subfamily of low-molecular-weight cytokines identified by their ability to attract and activate leukocytes. CC and CXC are two major structural variants that differ according to variations in a shared cysteine (C) motif. Accumulating laboratory evidence suggests that chemokines and chemokine receptors, such as CCL2/CCR2,[6] CX3CL1/CX3CR1,[7] CCR3,[8] and CXCR4[9] are involved in CNV. The CXC chemokine family has four highly conserved cysteine amino acid residues, with the first two cysteines separated by a nonconserved amino acid residue.[10] The NH2-terminus of several CXC chemokines contains three amino acid residues (Glu-Leu-Arg; "ELR" motif), which immediately precedes the first cysteine amino acid residue.[11] In general, the CXC chemokines, that are interferon-inducible and lack the ELR motif ("ELR-negative") inhibit angiogenesis, while the "ELR-positive" CXC chemokines promote angiogenesis.[11] A previous report has demonstrated that CXC ligands such as interferon-γ inducible protein 10-kDa (IP-10), monokine induced by interferon-γ (MIG), and interferon-inducible T cell α chemoattractant (I-TAC) are expressed in RPE.[12] However, their function in the retinal/choroidal angiogenesis remains largely unknown.

In the present study, using aged mice and mice with laser-induced CNV model, the expressions of 60 chemokines and chemokine receptors were investigated in DNA microarray analysis for the mouse eyes with laser-induced CNV. As a result, CXC chemokine receptor 3 (CXCR3) and one of its ligands were elevated in the CNV eyes compared with the control eyes. Using the mice lacking CXCR3 and neutralizing antibodies, the current study investigated the effect of CXCR3 on the CNV in the murine laser-induced CNV model.

Methods

Animals

All animal experiments followed the guidelines of the ARVO Statement for the Use of Animals in Ophthalmic and Vision Research. CXCR3-

From the Departments of [1]Ophthalmology and [2]Molecular Preventive Medicine, University of Tokyo School of Medicine, Tokyo, Japan.

Supported in part by grant aid from the Ministry of Education, Culture, Sports, Science, and Technology, Japan (#23592552).

Submitted for publication July 17, 2011; revised November 5, 2011, January 20 and February 9, 2012; accepted February 9, 2012.

Disclosure: **S. Fujimura**, None; **H. Takahashi**, None; **K. Yuda**, None; **T. Ueta**, None; **A. Iriyama**, None; **T. Inoue**, None; **T. Kaburaki**, None; **Y. Tamaki**, None; **K. Matsushima**, None; **Y. Yanagi**, None

Corresponding author: Yasuo Yanagi, Department of Ophthalmology, University of Tokyo School of Medicine, 7-3-1 Hongo, Bunkyo-ku, Tokyo 113-8655, Japan; yanagi-tky@umin.ac.jp.

deficient mice were prepared as described.[13,14] Genotypes were confirmed by PCR of genomic DNA extracted from tail snips. As mammalian CXCR3 gene is on the X chromosome and is a single copy in males, male wild-type C57BL/6 mice and female CXCR3-deficient mice (−/−) were mated to obtain male (Y/−) and female (+/−) offspring. Then, these male (Y/−) and female (+/−) mice were mated to get male (Y/+) and (Y/−) mice, and the male CXCR3-deficient (Y/−) mice and their CXCR3-competent (wild-type, Y/+) littermates were used for experiments.

Induction of CNV

The laser-induced model has become a common means of inducing experimental CNV since the original study in the rhesus monkey was performed.[15] For CNV induction, mice between 8 and 10 weeks of age were anesthetized by intraperitoneal injections (1000 μL/kg) of a mixture (7:3) of ketamine hydrochloride (Ketalar; Sankyo, Tokyo, Japan) and xylazine hydrochloride (Celactal; Bayer, Tokyo, Japan), and pupils were dilated with 0.5% tropicamide (Mydrin M; Santen Pharmaceutical, Osaka, Japan). Experimental CNV was created as has been described elsewhere.[16–20] Laser photocoagulations were applied to each eye between the major retinal vessels around the optic disc using a diode-laser photocoagulator (DC-3000; NIDEK, Osaka, Japan) with a slit-lamp delivery system (SL-7F; Topcon, Tokyo, Japan) at a spot size of 75 μm, duration of 0.02 second, and intensity of 200 mW. Laser photocoagulations were performed by a single operator (T.H.) in a masked manner. Production of a bubble at the time of laser exposure, which indicated rupture of Bruch's membrane, was confirmed for each lesion.

Microarray Analysis

Male 18-week-old mice were used for microarray analysis. Ten laser photocoagulations were applied to one eye, and the contralateral eye served as controls. Five days after laser treatment, messenger RNA (mRNA) from RPE-choroid fraction was isolated using RNeasy Mini kit (Qiagen Inc., Valencia, CA). Target RNA was hybridized on a GeneChip Mouse Genome 430 2.0 array (Affymetrix Inc, Santa Clara, CA) at the research Center for Advanced Science and Technology, University of Tokyo. The experimental procedures for the GeneChip were performed according to the Affymetrix technical manual. Paired sets of samples from individual animals were used for analysis ($n = 4$).

Immunohistochemistry

Immunohistochemical experiments were performed for murine laser-induced CNV.

For the histopathologic analysis of the murine CNV lesion, 10 applications of laser photocoagulation were delivered to both eyes of adult wild-type mouse. Eyes from the mice sacrificed with cervical dislocation 7 days after laser-photocoagulation were immediately enucleated and embedded in optimal cutting temperature compound (OCT, Sakura, Kobe, Japan) and snap-frozen. Transverse 10 μm sections were cut, collected on grass slides, fixed with acetone for 10 minutes, and stored at −80°C until use. Specific polyclonal rabbit antibodies against CXCR3 (1:200, Santa Cruz Biotechnology, Santa Cruz, CA) were used for the detection of CXCR3-expressing cells, and specific monoclonal rat antibodies against CD31 (1:100, BD Biosciences, Franklin Lakes, NJ) were used for the detection of vascular endothelial cells. The slides were incubated for 2 hours at room temperature with the first primary antibody. After washing, sections were incubated for 60 minutes in a solution of 1:300 secondary goat anti-rabbit antibodies conjugated to Alexa 488 (Invitrogen, Carlsbad, CA). After these first incubations, sections were incubated successively with the second primary antibody and 1:300 donkey anti-rat antibodies conjugated to Alexa 594 (Invitrogen). The slides were then washed, stained for 5 minutes with 4′,6-Diamino-2-Phenyl-Indole (DAPI; Sigma-Aldrich, St. Louis, MO) diluted 1:3000, washed again in PBS, then mounted in 1:1 glycerol-PBS. Negative immunohistochemistry controls were performed in parallel by using rabbit and rat isotype-matched IgG at the same concentrations as primary antibodies (i.e., negative control for anti-CXCR3 and anti-CD31). Immunoreactive cells were visualized, and images were recorded with a fluorescent microscope (model XI, Olympus, Tokyo, Japan).

Fluorescein Angiography (FA)

For the FA, three applications of laser photocoagulation were delivered to each eye of wild-type or CXCR3-deficient mouse ($n = 10$ per group). Seven days after the photocoagulation, FA was performed for quantitatively analyzing the amount of leakage from the CNV, as has been previously described.[16–19] Fluorescein sodium (10%, 0.1 mL/kg, Fluorescite; Alcon, Fort Worth, TX) was injected into the intraperitoneal cavity of the anesthetized mice. Four to six minutes after the injection, three angiograms were taken using a digital fundus camera (TRC-501X; Topcon), with a built-in filter for fluorescence. The images were captured with the built-in software (Imagenet; Topcon), imported to a Windows personal computer, and analyzed using Image-J software (National Institutes of Health, Bethesda, MD); the signal intensities (brightness) within the leakage from CNV were measured and integrated at each photocoagulated site. The FA evaluator was masked as to the genetic background of the mice and as to treatment.

FITC-Dextran Perfusion and CNV Size Measurement

The sizes of CNV lesions were measured in choroidal flatmounts as described.[17,21] Three to six hours after the FA, mice were re-anesthetized and perfused with 1 mL PBS containing 50 mg/mL fluorescein-labeled dextran (FITC-Dextran; Sigma-Aldrich) via the left ventricle. After the eyes were enucleated and briefly fixed in 4% paraformaldehyde (PFA), the anterior segment was removed, and the retina was carefully dissected from the eyecup. Four to six radial cuts were made from the edge to the equator, and the eyecup was flatmounted with the sclera facing down and examined by fluorescence microscopy (Olympus BX51). The images were digitized with a computer-controlled display camera and imported into a computer system. The area of CNV in the choroidal flatmounts was measured using the Image-J software. CNV lesions were identified as fluorescent blood vessels on the choroidal/retinal interface circumscribed by a region lacking fluorescence. The image analysis was performed with the observer masked to genetic background and to treatment.

Intravitreal Injection with Anti-CXCR3/Anti-IP-10 Neutralizing Antibody

Both eyes of the male adult (10 weeks old) wild-type mice were treated by laser as described above and separated randomly into three groups ($n = 8$–10 mice per group). Immediately after the laser treatment, the first group received 1 μg/2 μL of the control IgG (Southern Biotech Inc, Birmingham, AL), the second group received 1 μg/2 μL of the mouse anti-human CXCR3 neutral antibody (Abcam plc, Cambridge, UK), and the third group received 1 μg/2 μL of rabbit anti-mouse IP-10 neutral antibody (Abcam plc) in both eyes by intravitreal injection under systemic anesthesia and after pupil dilatation. Each agent was injected into the vitreous cavity 0.5 mm away from the limbus using a 5-μL syringe (Ito Corporation, Shizuoka, Japan) and a 33-gauge double-caliber needle (Ito Corporation) under a dissecting microscope. Then, CNV size and fluorescein leakage from it were evaluated 7 days after photocoagulation as described above.

Measurement of Macrophage Recruitment into CNV

To investigate the influence of CXCR3-deficiency on macrophage, which is supposed to have important role on CNV formation,[22] measurement of macrophage recruitment into CNV lesion was

performed for wild-type and CXCR3-deficient mouse, as previously described[23] with some modifications. The right eyes of male adult (10 weeks old) wild-type and CXCR3-deficient mice were treated by laser as described above (n = eight mice per group). Three applications of laser photocoagulation were delivered to each eye. Three days after the laser photocoagulations, all mice were sacrificed, and eyes were enucleated and briefly fixed in 4% PFA, and the choroidal flatmounts were made as described above. After blocking with 5% goat-serum, these choroidal flatmounts were incubated with 1:100 rat anti-mouse F4/80 antibody conjugated to Alexa 488 (Life Technologies, Carlsbad, CA), then washed and examined by fluorescence microscopy (Olympus BX51). The F4/80-positive cells inside or around each laser photocoagulation site were counted and averaged for total of three laser photocoagulation sites of each eye. Negative control staining was also performed in parallel for one additional laser-treated eye of wild-type and CXCR3-deficient mouse by using rat isotype-matched IgG conjugated to Alexa 488 at the same concentration.

Real-Time RT-PCR

For the further quantitative analysis of mRNA expressions in RPE-choroid fractions of mouse eyes, real-time RT-PCR analyses were performed. The expressions of CXCR3 and its three main ligands (IP-10, MIG, and I-TAC) were quantified in laser-induced CNV model of wild-type mice, and several cytokines and molecules relevant to CNV,[6,24–26] vascular endothelial growth factor (VEGF), pigment epithelium-derived factor (PEDF), C-C chemokine ligand-2 (CCL2), and complement component-3 (C3) were quantified in laser-induced CNV model to compare these expressions in wild-type mice with CXCR3-deficient mice. For the real-time RT-PCR, 10 applications of photocoagulation were delivered to each eye of wild-type or CXCR3-deficient mouse. Three days after laser-treatment, when the expression of these cytokines and molecules reaches its peak (Ref. 27 and Takahashi H, unpublished data, 2010), mice were sacrificed by cervical dislocation, and eyes were harvested immediately. RPE-choroid fractions were isolated from the controls and the CNV eyes and were stored at −80°C until use. RNA from the RPE-choroid fractions was isolated using an SV Total RNA Isolation Kit (Promega, Madison, WI) in accordance with the manufacturer's instructions. The cDNA was prepared using Superscript III for RT-PCR (Invitrogen). Each PCR was carried out in a 20-μL volume using Platinum SYBR Green qPCR SuperMix UDG (Invitrogen) for 15 minutes at 95°C denature, followed by 55 cycles at 95°C for 30 seconds and 60°C for 1 minute in Roche Light Cycler. Values for each gene were normalized to expression levels of glyceraldehyde 3-phosphate dehydrogenase (GAPDH). The sequences of the primers used for RT-PCR were as follows: mouse-GAPDH, left, 5′-aactttggcattgtggaagg-3′, right, 5′-cacattgggggtaggaacac-3′; mouse-CXCR3, left, 5′-gctgtagccgatgttctgctggtg-3′, right, 5′-tgcactatgctcagatatctgtc-3′; mouse-IP10, left, 5′-cccacgtgttgagatcattg-3′, right, 5′-cactgggtaaaggggagtga-3′; mouse-MIG, left, 5′-aaaatttcatcacgcccttg-3′, right, 5′-tctccagcttggtgaggtct-3′; mouse-I-TAC, left, 5′-agtaacggctgcgacaaagt-3′, right, 5′-gcatgttccaagacagcaga-3′; mouse-VEGF, left, 5′-gtacctccaccatgccaagt-3′, right, 5′-gcattcacatctgctgtgct-3′; mouse-PEDF, left, 5′-cacccgacttcagcaagattact-3′, right, 5′-tcgaaagcagccctgtgtt-3′; mouse-CCL2, left, 5′-tctggacccattccttcttg-3′, right, 5′-caggtccctgtcatgcttct-3′; and mouse-C3, left, 5′-ccgcaggctgtggggaacag-3′, right, 5′-gctgtcagccaggtgctggg-3′. Ten samples were used for each analysis.

Statistical Analysis

The results of the real-time RT-PCR and macrophage recruitment were analyzed by the Mann-Whitney U test. The fluorescein leakage and the integrated area of the CNV specimen, which were obtained from the three CNV lesions in each eye, were averaged so that one value for each eye was used for analysis. In order to homogenize the variance, which increases as lesion size increases, the natural logarithms of all data, including the fluorescein leakage and the integrated area of CNV, were used for analysis as has been described in a previous report.[28] The nested ANOVA test was performed to compare the fluorescein leakage or CNV area between two groups of mice; P values less than 0.05 were considered statistically significant.

Results

Microarray Analysis of Chemokines or Chemokine Receptors in CNV

To investigate which chemokines or chemokine receptors have significant association with the AMD pathogenesis, we used microarray analysis, focusing on 60 transcripts of chemokine, chemokine receptor, and chemokine-like factor, for laser-induced CNV model mice. The results demonstrated that at the mRNA level, 23 molecules were up-regulated in the laser-treated eyes (Table 1). Among these up-regulated molecules, CCL2, CXCL4, CCR1, CCR2, CXCL5, CCL11, CXCL10, CXCR3, CXCL12, CXCR4, and CXCL1 were supposed to have angiogenic or angiostatic functions in previous reports.[10,29] Among the 11 molecules, CCL2/CCR2, CXCL12/CXCR4, and CCL11 were already reported to have some effects on CNV.[6–9] Therefore, in the current study, interest was focused on CXCR3 and one of its ligands, CXCL10 (IP-10), because to the best of the authors' knowledge, their role in CNV development had never been investigated, and it has been suggested that CXCR3 is relevant to angiostasis in previous studies.[30–33]

Expression of CXCR3 and Three Major Ligands in CNV

CXCR3 is one of the mammalian chemokine receptors, promoting chemotaxis and cell proliferation, binding with its three major chemokines: IP-10, MIG, and I-TAC. Real-time RT-PCR analysis for CXCR3 was performed to identify their expression on the murine experimental CNV, which revealed increased expression of CXCR3 in the RPE-choroid fractions of laser-treated eyes compared with nontreated fellow eyes (Figs. 1A, 1B). The levels of IP-10 mRNA were up-regulated in the CNV eyes compared with the naïve eyes, while the other two major ligands of CXCR3, MIG, and I-TAC had not changed (Fig. 1C). Additionally, immunohistochemical analysis of murine experimental CNV revealed positive CXCR3 expressions in the endothelial cells of CNV (Fig. 2).

CXCR3-Deficiency or Inhibition of CXCR3/IP-10 Exacerbates Laser-Induced CNV

Histological analysis has demonstrated that CXCR3-deficient mice showed no abnormalities of retinal structure including retinal and choroidal vessels (data not shown). Using the CXCR3-deficient mice, experiments were performed to investigate whether CXCR3 has a role in CNV. The leakage from the CNV and CNV size were analyzed by FA and choroidal flatmount, respectively. The results demonstrated that, at 1 week after laser photocoagulation, FA showed significantly greater leakage in CXCR3-deficient mice than in wild-type mice ($n = 10$ per group, $P < 0.01$, Fig. 3A). Additionally, the analysis of choroidal flatmounts showed CXCR3-deficient mice developed larger size CNV than wild-type mice ($P < 0.01$, Fig. 3B).

To confirm the presumed CXCR3 function as anti-CNV development, further experiments were performed using anti-CXCR3 neutral antibody and anti-IP-10 neutral antibody. As a result, FA showed that both groups of the eyes that received intravitreal anti-CXCR3 neutral antibody injection and the eyes that received anti-IP10 neutral antibody injection developed greater leakage from the CNV than eyes that received control IgG ($P < 0.05$ and $P < 0.01$, respectively, Fig. 3C). The

Table 1. Up-Regulated Genes in Laser-Treated Mouse Eyes Compared with Nontreated Fellow Eyes

Unigene	Gene Name	Abbreviations	Fold Change
Mm_137	C-C chemokine ligand 6	CCL6	5.51
Mm_867	C-C chemokine ligand 12	CCL12	4.53
Mm_290,320	C-C chemokine ligand 2	CCL2	3.92
Mm_332,490	C-X-C chemokine ligand 4	CXCL4	3.88
Mm_14,302	C-C chemokine receptor 5	CCR5	3.53
Mm_41,988	C-C chemokine ligand 17	CCL17	3.37
Mm_274,927	C-C chemokine receptor 1	CCR1	3.24
Mm_341,574	C-C chemokine ligand 7	CCL7	3.11
Mm_6272	C-C chemokine receptor 2	CCR2	2.93
Mm_42,029	C-C chemokine ligand 8	CCL8	2.77
Mm_4660	C-X-C chemokine ligand 5	CXCL5	2.37
Mm_4686	C-C chemokine ligand 11	CCL11	2.10
Mm_877	C-X-C chemokine ligand 10	CXCL10 (IP-10)	2.04
Mm_12,876	C-X-C chemokine receptor 3	CXCR3	1.89
Mm_277,129	C-X-C chemokine ligand 16	CXCL16	1.79
Mm_29,658	Chemokine-like factor super family 3		1.72
Mm_143,745	C-C chemokine ligand 28	CCL28	1.55
Mm_303,231	C-X-C chemokine ligand 12	CXCL12	1.53
Mm_1401	C-X-C chemokine receptor 4	CXCR4	1.36
Mm_35,600	Chemokine-like factor super family 7		1.29
Mm_10,116	C-X-C chemokine ligand 13	CXCL13	1.25
Mm_21,013	C-X-C chemokine ligand 1	CXCL1	1.20
Mm_7275	C-C chemokine ligand 25	CCL25	1.13

Genes are ranked from high to low fold change (differential expression in laser-treated eye versus normal eye). Among other 37 molecules, seven molecules are not up-regulated, and 30 molecules are not detected.

measurement of CNV size also showed that both groups of the eyes that received anti-CXCR3 antibody and the eyes that received anti-IP10 antibody developed larger CNV than the eyes injected with control IgG ($P < 0.01$, Fig. 3D).

Measurement of F4/80-positive cells infiltrating inside or around CNV lesion revealed that more macrophages are recruited to CNV lesion of CXCR3-deficient mouse than that of wild-type mouse (42 ± 8 vs. 22 ± 7 counts/photocoagula-

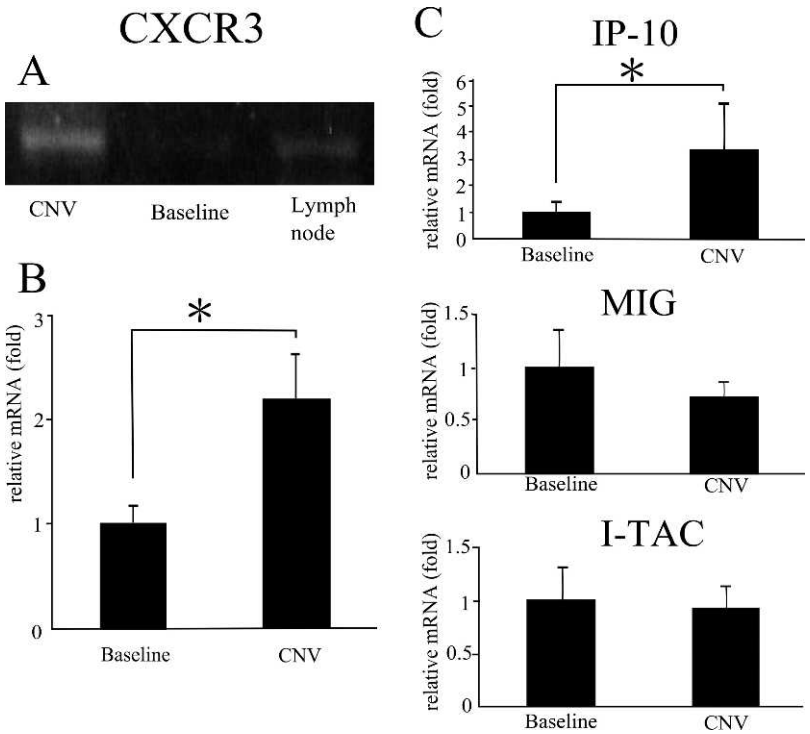

Figure 1. Messenger-RNA expression of CXCR3 and its three ligands in mouse eyes. (**A**, **B**) CXCR3 mRNA expression in the RPE-choroid fraction of laser-induced CNV eye is increased from that of naïve eye (Baseline). (**A**) An aliquot of each PCR reaction is electrophoresed on 1.5% agarose gel and visualized with ethidium bromide. Murine lymph node is used as positive control. (**B**) Real-time RT-PCR also demonstrates the increased expression of CXCR3 in mouse eye with CNV. (**C**) Expressions of interferon-γ IP-10, MIG, and I-TAC mRNA in the RPE-choroid fractions of mouse experimental CNV. The expression levels are normalized over GAPDH levels and expressed as n-fold increases. *$P < 0.05$ by Mann-Whitney U test.

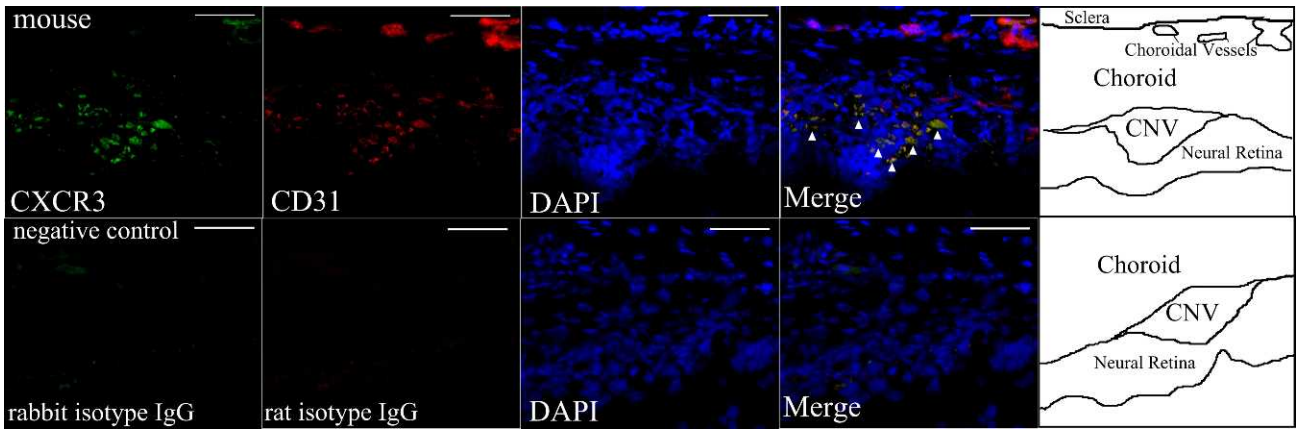

Figure 2. Immunohistochemical staining with anti-CXCR3 antibody for mouse experimental CNV. Double-staining (upper row) with anti-CXCR3 antibody and anti-CD31 antibody shows that CXCR3 immunoreactivity is present at endothelium of mouse CNV (*arrowheads*), whereas negative control stain (lower row) shows no positive staining. Scale bar: 50 μm.

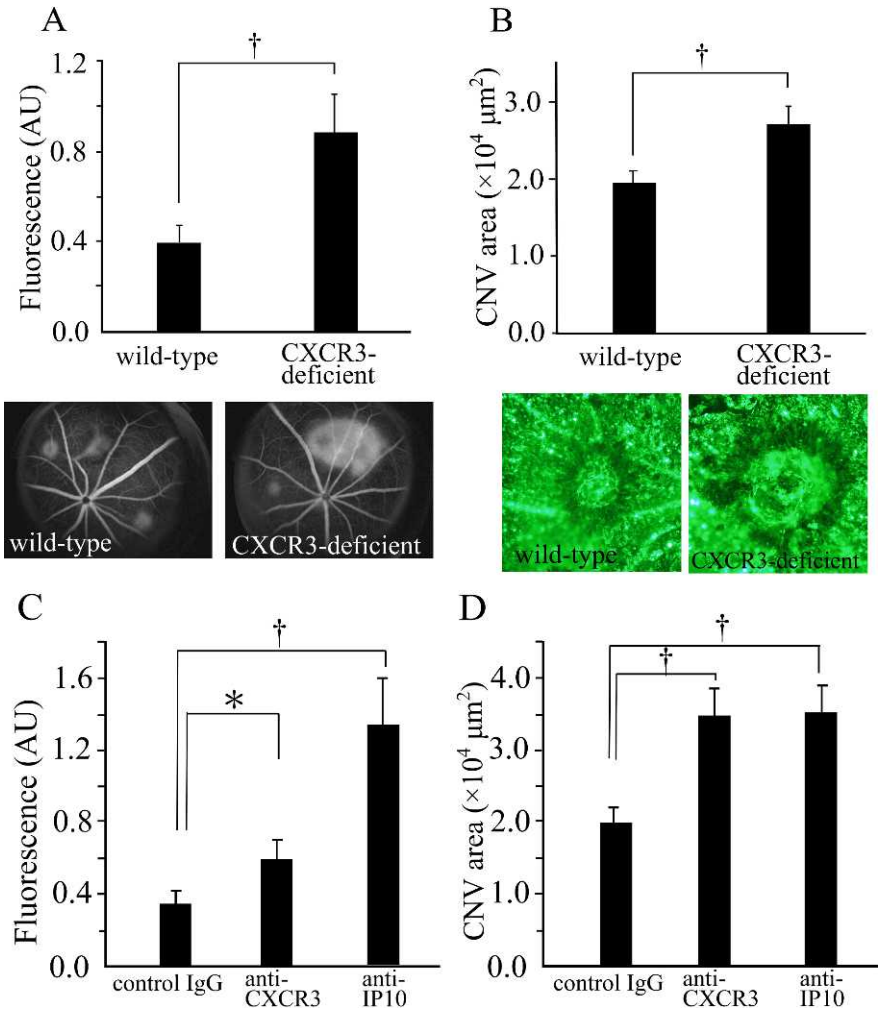

Figure 3. The quantification of laser-induced CNV in wild-type (Y/+), CXCR3-deficient (Y/−) mice, wild-type mice treated with anti-CXCR3 neutral antibody or anti-IP-10 neutral antibody. (**A**) Fluorescin angiography demonstrates greater leakage from CNV in CXCR3-deficient mice compared with wild-type mice. (**B**) Quantification of CNV size by choroidal flat mounts shows that CNV lesions are larger in CXCR3-deficient mice than that in wild-type mice. Representative images of fluorescein angiogram and choroidal flatmounts of wild-type and CXCR3-deficient mice were shown under the graphs. (**C**, **D**) Wild-type mice treated with intravitreal injection of anti-CXCR3 neutral antibody or anti-IP-10 neutral antibody develop larger CNV with greater leakage compared with mice treated with control IgG. †$P < 0.01$, *$P < 0.05$ by nested-ANOVA.

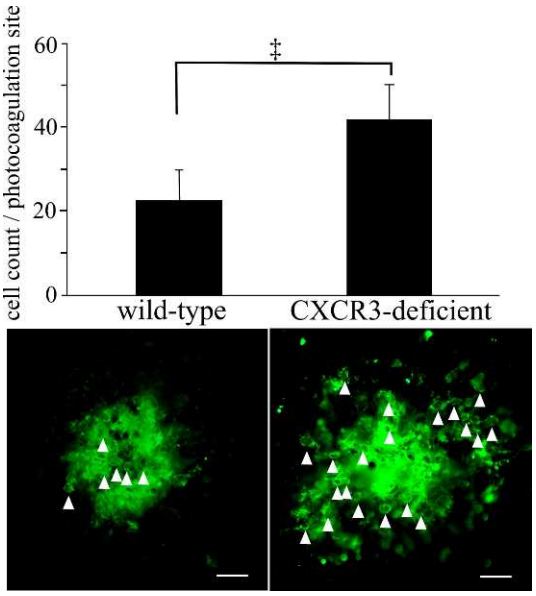

Figure 4. Macrophage recruitment into CNV lesions of CXCR3-deficient and wild-type mice 3 days after laser photocoagulation. Quantification of F4/80-positive cells/photocoagulation site reveals that more macrophages are recruited to CNV lesions of CXCR3-deficient mice than those of wild-type mice (‡$P < 0.01$ by Mann-Whitney *U* test). Representative images of F4/80-positive cells (*arrowheads*) inside or around laser burns on choroidal flatmounts of wild-type and CXCR3-deficient mice were shown under the graphs. Scale bar: 50 μm.

tion site, $P < 0.01$, Fig. 4). Negative control staining performed for additional flatmounts showed negative staining (data not shown).

Messenger-RNA Expressions of Several Cytokines in Laser-Treated Eyes of CXCR3-Deficient and Wild-Type Mice

To investigate the expression of factors associated with CNV formation, the real-time RT-PCR analysis was performed for RPE-choroid tissues of CXCR3-deficient and wild-type mice. In good accordance with previous studies,[24–26,34] 3 days after laser photocoagulation, elevation of cytokines and molecules, such as VEGF, PEDF, CCL2, and C3, were observed, from baseline ($P < 0.05$ versus baseline: Figs. 5A–5D). There was no difference in VEGF, PEDF, and C3 expression between CXCR3-deficient and wild-type mice both at baseline and after laser photocoagulation. However, the CCL2 expression of CXCR3-deficient mice was significantly higher than that of wild-type mice after laser photocoagulation (Fig. 5C). The ratio of VEGF to PEDF increased by 2.14-fold in average in wild-type mice ($P < 0.05$ versus baseline), and increased by 2.93-fold in average in CXCR3-deficient mice ($P < 0.05$ versus baseline) after laser photocoagulation with statistically no significant difference between the two groups.

Discussion

To the best of our knowledge, the current study showed relationships between CXCR3 and CNV formation for the first time. The results demonstrated the positive expression of CXCR3 on vascular endothelial cells of CNV, corroborating previous studies demonstrating CXCR3 expression on murine and human endothelium of newly formed blood vessels[30,31,35] or the endothelial cell line.[36] It is also worth mentioning that immunohistochemical staining of human CNV obtained in surgical procedure also showed positive staining on CNV with anti-CXCR3 antibody (data not shown). In the present study, IP-10 mRNA was up-regulated in laser-treated mouse eyes, which was compatible with the clinical results that showed elevation of serum concentration of IP-10 in patients with AMD and immunohistochemical detection of IP-10 in AMD eyes, especially within the neovascular membrane.[37] These observations, together with the current results, suggest that CXCR3 and/or IP-10 could be an important pathogenic factor during development of CNV.

CXCR3 has seven transmembrane G-protein-coupled structures. Accumulating evidence suggests that CXCR3 is anti-angiogenic.[10,11,30–33,35] Human CXCR3 has two splice variants with opposite functions: CXCR3-A and CXCR3-B. CXCR3-A is mainly expressed on the surface of type-1 helper T cells (Th1) and natural killer (NK) cells. Human CXCR3-B is expressed on the endothelial cells of new vessels in healing wounds or

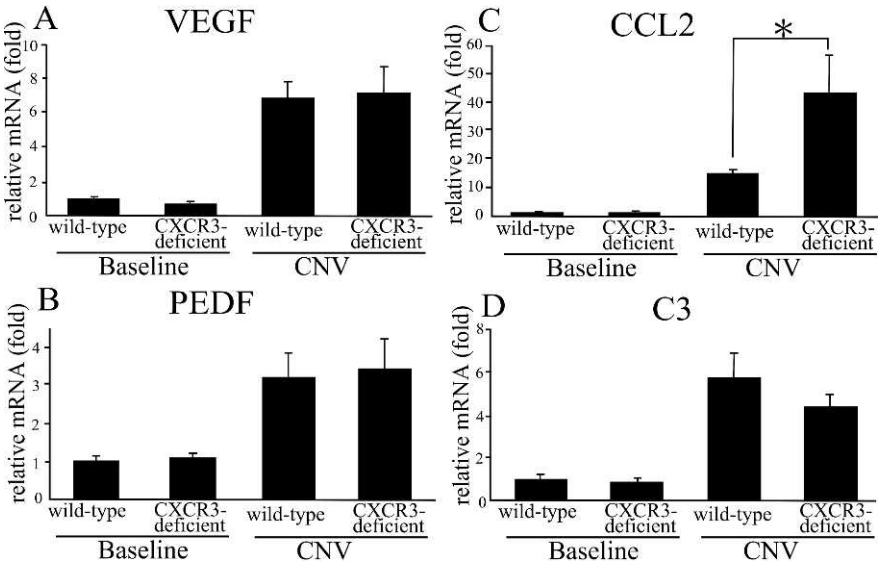

Figure 5. Expressions of VEGF, PEDF, CCL2, and C3 mRNA in RPE-choroid fraction of naïve (Baseline) eyes and laser-treated (CNV) eyes of wild-type mice and CXCR3-deficient mice. All amounts were expressed as n-fold increases from wild-type naïve eye. *$P < 0.05$ by Mann-Whitney *U* test.

tumors, inhibiting angiogenesis and tumorgenesis, acting with the three major ligands (IP-10, MIG, and I-TAC).[31,32,38] Although these splice variants of CXCR3 do not exist in mice,[39] CXCR3 was originally identified on murine endothelial cells,[40] and CXCR3 and IP-10 showed angiostatic effects in some rodent models.[30,41,42] A previous study[30] has demonstrated that CXCR3-deficient mice develop a significantly greater number of vessels in wounded tissue.

Intravitreal injection of mouse recombinant IP-10 for laser-treated eyes of wild-type mice, however, failed to show a significant effect in the leakage/size of murine experimental CNV (data not shown). On the contrary, intravitreal administration with IP-10 neutral antibodies exacerbated murine CNV, as described above. From these results, it is rational to consider that exogenous administration with IP-10 could not attenuate CNV because endogenous IP-10 might be up-regulated to saturation level after laser treatment.

The molecular mechanism underlying the anti-angiogenic function of CXCR3 remains unknown. A previous report in vitro[33] suggested that IP-10 inhibits VEGF-mediated m-calpain activation, thereby disrupting newly formed vessels via CXCR3 signaling. The present results showed that there were no differences in the VEGF expressions in the laser-induced CNV between CXCR3-deficient and wild-type mice. This suggests that CXCR3-mediated angiostasis was independent of the VEGF-signaling pathway. Similarly, it is likely that the mechanism of the CXCR3 effect on CNV might be independent of PEDF or C3 because both of these mRNA expressions showed no difference between CXCR3-deficient and wild-type mouse.

Alternatively, CXCR3 could contribute to angiostasis via other mechanisms. CXCR3 and its ligands promote Th1-dependent immunity through recruitment of CXCR3-expressing T and NK cells to inhibit angiogenesis, which mechanism has been described as "immunoangiostasis."[43,44] In some previous studies with animal models of non-small-cell lung cancer, investigators showed the inhibition of Th1 cytokine-induced cell-mediated immunity resulted in the inhibition of tumor-associated angiogenesis and the suppression of tumor growth.[45,46] It is possible that the lack of this process in the CXCR-deficient mice or mouse eyes injected with anti-CXCR3/anti-IP10 neutralizing antibody played a part in the CNV exacerbation. It is difficult to discriminate, however, between the direct anti-angiogenic effect through CXCR3 on endothelial cells and indirect mechanism through the recruitment of CXCR3-expressing T and NK cells.

In the present study, macrophage infiltration into the CNV lesion and CCL2 expression in laser-treated eyes of CXCR3-deficient mice were higher than those of wild-type mice. In CNV formation, the chemokine that has generated particular interest is CCL2 and its receptor CCR2.[6,47] CCR2 is a chemokine receptor found on macrophages that bind the CCL2 chemokine. Deficiencies in CCR2 lead to decreased leukocyte adhesion to microvasculature, as well as decreased extravasation of monocyte from the circulatory system into surrounding tissues.[22] These recent evidences suggest that CCL2 might play a role in monocyte and microglial cell recruitment. Moreover, a recent clinical study[34] suggests that elevated intraocular CCL2 levels are associated with exudative AMD. According to the current results, together with the previous investigations that show the relation between CCL2/CCR2 and macrophage,[22,48] it is possible that enhanced recruitment of macrophages and/or CCL2 elevation in the CXCR3-deficient mice might play a role in developing larger CNV in the CXCR3-deficient mice. In respect of leukocyte immunity, CCL2 is mainly associated with monocytes, while CXCR3 is mainly associated with Th1 cell.[49] An important issue for future research is to determine whether the up-regulated expression of CCL2 in the CXCR3-deficient mice is the epiphenomenon of the increased laser-induced CNV size or whether there is crosstalk between the CXCR3-mediated signaling pathway and the expression of CCL2.

In conclusion, these findings demonstrate that CXCR3-signaling of CNV endothelial cells or that mediating immunoangiostasis could inhibit the CNV formation. Further experimental approach for CXCR3 and its ligands would allow the development of new effective therapeutic strategies for AMD.

References

1. Crabb JW, Miyagi M, Gu X, et al. Drusen proteome analysis: an approach to the etiology of age-related macular degeneration. *Proc Natl Acad Sci U S A*. 2002;99:14682–14687.
2. Marin-Castano ME, Csaky KG, Cousins SW. Nonlethal oxidant injury to human retinal pigment epithelium cells causes cell membrane blebbing but decreased MMP-2 activity. *Invest Ophthalmol Vis Sci*. 2005;46:3331–3340.
3. Hageman GS, Luthert PJ. Victor Chong NH, Johnson LV, Anderson DH, Mullins RF. An integrated hypothesis that considers drusen as biomarkers of immune-mediated processes at the RPE-Bruch's membrane interface in aging and age-related macular degeneration. *Prog Retin Eye Res*. 2001;20:705–732.
4. Mullins RF, Aptsiauri N, Hageman GS. Structure and composition of drusen associated with glomerulonephritis: implications for the role of complement activation in drusen biogenesis. *Eye (Lond)*. 2001;15:390–395.
5. Mullins RF, Russell SR, Anderson DH, Hageman GS. Drusen associated with aging and age-related macular degeneration contain proteins common to extracellular deposits associated with atherosclerosis, elastosis, amyloidosis, and dense deposit disease. *FASEB J*. 2000;14:835–846.
6. Ambati J, Anand A, Fernandez S, et al. An animal model of age-related macular degeneration in senescent Ccl-2- or Ccr-2-deficient mice. *Nat Med*. 2003;9:1390–1397.
7. Tuo J, Bojanowski CM, Zhou M, et al. Murine ccl2/cx3cr1 deficiency results in retinal lesions mimicking human age-related macular degeneration. *Invest Ophthalmol Vis Sci*. 2007;48:3827–3836.
8. Takeda A, Baffi JZ, Kleinman ME, et al. CCR3 is a target for age-related macular degeneration diagnosis and therapy. *Nature*. 2009;460:225–230.
9. Sengupta N, Afzal A, Caballero S, et al. Paracrine modulation of CXCR4 by IGF-1 and VEGF: implications for choroidal neovascularization. *Invest Ophthalmol Vis Sci*. 51:2697–2704.
10. Belperio JA, Keane MP, Arenberg DA, et al. CXC chemokines in angiogenesis. *J Leukoc Biol*. 2000;68:1–8.
11. Strieter RM, Polverini PJ, Kunkel SL, et al. The functional role of the ELR motif in CXC chemokine-mediated angiogenesis. *J Biol Chem*. 1995;270:27348–27357.
12. Shi G, Maminishkis A, Banzon T, et al. Control of chemokine gradients by the retinal pigment epithelium. *Invest Ophthalmol Vis Sci*. 2008;49:4620–4630.
13. Yoneyama H, Matsuno K, Toda E, et al. Plasmacytoid DCs help lymph node DCs to induce anti-HSV CTLs. *J Exp Med*. 2005;202:425–435.
14. Hancock WW, Lu B, Gao W, et al. Requirement of the chemokine receptor CXCR3 for acute allograft rejection. *J Exp Med*. 2000;192:1515–1520.
15. Ryan SJ. The development of an experimental model of subretinal neovascularization in disciform macular degeneration. *Trans Am Ophthalmol Soc*. 1979;77:707–745.
16. Takahashi H, Obata R, Tamaki Y. A novel vascular endothelial growth factor receptor 2 inhibitor, SU11248, suppresses

choroidal neovascularization in vivo. *J Ocul Pharmacol Ther*. 2006;22:213–218.

17. Takahashi H, Yanagi Y, Tamaki Y, Uchida S, Muranaka K. COX-2-selective inhibitor, etodolac, suppresses choroidal neovascularization in a mice model. *Biochem Biophys Res Commun*. 2004;325:461–466.
18. Yanagi Y, Tamaki Y, Obata R, et al. Subconjunctival administration of bucillamine suppresses choroidal neovascularization in rat. *Invest Ophthalmol Vis Sci*. 2002;43:3495–3499.
19. Yanagi Y, Tamaki Y, Inoue Y, Obata R, Muranaka K, Homma N. Subconjunctival doxifluridine administration suppresses rat choroidal neovascularization through activated thymidine phosphorylase. *Invest Ophthalmol Vis Sci*. 2003;44:751–754.
20. Kami J, Muranaka K, Yanagi Y, Obata R, Tamaki Y, Shibuya M. Inhibition of choroidal neovascularization by blocking vascular endothelial growth factor receptor tyrosine kinase. *Jpn J Ophthalmol*. 2008;52:91–98.
21. Edelman JL, Castro MR. Quantitative image analysis of laser-induced choroidal neovascularization in rat. *Exp Eye Res*. 2000;71:523–533.
22. Tsutsumi C, Sonoda KH, Egashira K, et al. The critical role of ocular-infiltrating macrophages in the development of choroidal neovascularization. *J Leukoc Biol*. 2003;74:25–32.
23. Jasielska M, Semkova I, Shi X, et al. Differential role of tumor necrosis factor (TNF)-alpha receptors in the development of choroidal neovascularization. *Invest Ophthalmol Vis Sci*. 51:3874–3883.
24. Ishibashi T, Hata Y, Yoshikawa H, Nakagawa K, Sueishi K, Inomata H. Expression of vascular endothelial growth factor in experimental choroidal neovascularization. *Graefes Arch Clin Exp Ophthalmol*. 1997;235:159–167.
25. Renno RZ, Youssri AI, Michaud N, Gragoudas ES, Miller JW. Expression of pigment epithelium-derived factor in experimental choroidal neovascularization. *Invest Ophthalmol Vis Sci*. 2002;43:1574–1580.
26. Bora PS, Sohn JH, Cruz JM, et al. Role of complement and complement membrane attack complex in laser-induced choroidal neovascularization. *J Immunol*. 2005;174:491–497.
27. Rohrer B, Long Q, Coughlin B, et al. A targeted inhibitor of the alternative complement pathway reduces angiogenesis in a mouse model of age-related macular degeneration. *Invest Ophthalmol Vis Sci*. 2009;50:3056–3064.
28. Takahashi H, Tamaki Y, Ishii N, et al. Identification of a novel vascular endothelial growth factor receptor 2 inhibitor and its effect for choroidal neovascularization in vivo. *Curr Eye Res*. 2008;33:1002–1010.
29. Kiefer F, Siekmann AF. The role of chemokines and their receptors in angiogenesis. *Cell Mol Life Sci*. 68:2811–2830.
30. Bodnar RJ, Yates CC, Rodgers ME, Du X, Wells A. IP-10 induces dissociation of newly formed blood vessels. *J Cell Sci*. 2009; 122:2064–2077.
31. Lasagni L, Francalanci M, Annunziato F, et al. An alternatively spliced variant of CXCR3 mediates the inhibition of endothelial cell growth induced by IP-10, Mig, and I-TAC, and acts as functional receptor for platelet factor 4. *J Exp Med*. 2003;197: 1537–1549.
32. Yang J, Richmond A. The angiostatic activity of interferon-inducible protein-10/CXCL10 in human melanoma depends on binding to CXCR3 but not to glycosaminoglycan. *Mol Ther*. 2004;9:846–855.
33. Bodnar RJ, Yates CC, Wells A. IP-10 blocks vascular endothelial growth factor-induced endothelial cell motility and tube formation via inhibition of calpain. *Circ Res*. 2006;98:617–625.
34. Jonas JB, Tao Y, Neumaier M, Findeisen P. Monocyte chemoattractant protein 1, intercellular adhesion molecule 1, and vascular cell adhesion molecule 1 in exudative age-related macular degeneration. *Arch Ophthalmol*. 128:1281–1286.
35. Romagnani P, Annunziato F, Lasagni L, et al. Cell cycle-dependent expression of CXC chemokine receptor 3 by endothelial cells mediates angiostatic activity. *J Clin Invest*. 2001;107:53–63.
36. Salcedo R, Resau JH, Halverson D, et al. Differential expression and responsiveness of chemokine receptors (CXCR1-3) by human microvascular endothelial cells and umbilical vein endothelial cells. *FASEB J*. 2000;14:2055–2064.
37. Mo FM, Proia AD, Johnson WH, Cyr D, Lashkari K. Interferon gamma-inducible protein-10 (IP-10) and eotaxin as biomarkers in age-related macular degeneration. *Invest Ophthalmol Vis Sci*. 51:4226–4236.
38. Feldman ED, Weinreich DM, Carroll NM, et al. Interferon gamma-inducible protein 10 selectively inhibits proliferation and induces apoptosis in endothelial cells. *Ann Surg Oncol*. 2006;13:125–133.
39. Campanella GS, Colvin RA, Luster AD. CXCL10 can inhibit endothelial cell proliferation independently of CXCR3. *PLoS One*. 5:e12700.
40. Soto H, Wang W, Strieter RM, et al. The CC chemokine 6Ckine binds the CXC chemokine receptor CXCR3. *Proc Natl Acad Sci U S A*. 1998;95:8205–8210.
41. Luster AD, Cardiff RD, MacLean JA, Crowe K, Granstein RD. Delayed wound healing and disorganized neovascularization in transgenic mice expressing the IP-10 chemokine. *Proc Assoc Am Physicians*. 1998;110:183–196.
42. Yates CC, Whaley D, Kulasekeran P, et al. Delayed and deficient dermal maturation in mice lacking the CXCR3 ELR-negative CXC chemokine receptor. *Am J Pathol*. 2007;171: 484–495.
43. Balestrieri ML, Balestrieri A, Mancini FP, Napoli C. Understanding the immunoangiostatic CXC chemokine network. *Cardiovasc Res*. 2008;78:250–256.
44. Pan J, Burdick MD, Belperio JA, et al. CXCR3/CXCR3 ligand biological axis impairs RENCA tumor growth by a mechanism of immunoangiostasis. *J Immunol*. 2006;176:1456–1464.
45. Sharma S, Yang SC, Hillinger S, et al. SLC/CCL21-mediated antitumor responses require IFNgamma, MIG/CXCL9 and IP-10/CXCL10. *Mol Cancer*. 2003;2:22.
46. Hillinger S, Yang SC, Zhu L, et al. EBV-induced molecule 1 ligand chemokine (ELC/CCL19) promotes IFN-gamma-dependent antitumor responses in a lung cancer model. *J Immunol*. 2003;171:6457–6465.
47. Yamada K, Sakurai E, Itaya M, Yamasaki S, Ogura Y. Inhibition of laser-induced choroidal neovascularization by atorvastatin by downregulation of monocyte chemotactic protein-1 synthesis in mice. *Invest Ophthalmol Vis Sci*. 2007;48:1839–1843.
48. Luhmann UF, Robbie S, Munro PM, et al. The drusenlike phenotype in aging Ccl2-knockout mice is caused by an accelerated accumulation of swollen autofluorescent subretinal macrophages. *Invest Ophthalmol Vis Sci*. 2009;50:5934–5943.
49. Sallusto F, Lenig D, Mackay CR, Lanzavecchia A. Flexible programs of chemokine receptor expression on human polarized T helper 1 and 2 lymphocytes. *J Exp Med*. 1998; 187:875–883.